

Exergetic Performance Evaluation and Comparative Study of A Roughened Solar Air Heater using MATLAB

Ankit Kumar ¹,

¹ CSIR-Indian Institute of Petroleum,
Dehradun, Uttarakhand, 248005,
India

Vijay Singh Bisht ²

²Department Of Thermal Engineering,
Faculty of Technology, Uttarakhand Technical University,
Dehradun 248007, Uttarakhand, India

Abstract- A comparative study based on exergetic performance of two different types of artificial roughness geometries on the absorber plate of solar air heater has been presented. The performance evaluation in terms of thermal efficiency (η_{th}), effective efficiency (η_{eff}), exergetic efficiency (η_{ex}) and different exergy loss parameters has been carried out analytically, for various values of temperature rise parameter ($\Delta T/I$) and relative roughness height (e/D). The second law based exergy analysis is suitable for design of rib roughened solar air heaters as it incorporates quality of useful energy output and pumping power. The two roughness geometries are discrete W-shape rib roughness and W-shape rib roughness have been selected. The correlations for heat transfer and coefficient of friction developed by respective investigators have been used to calculate efficiencies. It was investigated that discrete W-shape rib roughness has better thermal efficiency (η_{th}), effective efficiency (η_{eff}) and exergetic efficiency (η_{ex}) as compared to the W-shape rib roughness. The optimum parameters are relative roughness height (e/D) of 0.3375 at an angle of attack of 60° and isolation value of 1000 w/m^2 . It was investigated that discrete W-shaped rib roughness has 33% more exergetic efficiency than W-shaped rib roughness under similar performance parameters such as aspect ratio (8), relative roughness height (e/D) of 0.3375, angle of attack (α) of 60° , relative roughness pitch (P/e) of 10 and isolation value of 1000 w/m^2 with Reynolds number ranges from 4000 to 14000. Curves of thermal efficiency (η_{th}), effective efficiency (η_{eff}), exergetic efficiency (η_{ex}) and different exergy loss parameters with respect to temperature rise parameter ($\Delta T/I$) and relative roughness height (e/D) are also plotted.

Keywords- Exergetic efficiency, MATLAB, Artificial roughness, Solar air heater, W and discrete W shape roughness.

1. INTRODUCTION

Energy is defined as the universal measure of work for human, nature and machine. It is basically an input to everything to perform work however it also refers to a condition or state of matter. Energy is a basic ingredient to the recipe of day to day life. Solar energy, one of the sources of renewable energy, is the only energy whose small amount supplies a lot of energy. It is clean and most plentiful energy resource among renewable energy resources. Solar energy is universally available source of

inexhaustible energy but the major drawbacks of this energy are that it is a dilute form of energy, which is available sporadically and uncertainly. Solar air heaters are mostly acceptable because of their simplicity in structure, functioning and most widely used solar energy collector device (i.e., [1]). These are the device which converts solar energy into thermal energy which is used for various purposes. They are less efficient because of low convective heat transfer coefficient value between absorber plate and flowing air. Their efficiency can be increased with the provision of roughness that can break laminar sub layer. Due to this artificial roughness local turbulence is created which helps in increasing the amount of heat transfer. Numerous study of artificial roughness attributed largely in the field of solar air heater to enhance their performance. Important phenomena responsible for heat transfer enhancement in solar air heater are enhanced turbulence, generation of secondary flows, flow separations and reattachments and mixing. Initial investigated roughness are transverse wires (i.e., [2,3]) V-up (i.e., [4]), (transverse, inclined, V-up and V-down) (i.e., [5]), arc shaped (i.e., [6]) and multiple V-rib (i.e., [7]). They contributed

Nomenclature			
A_p	Surface area of absorber plate/collector, m^2	ΔT	Temperature rise across duct
D	Equivalent hydraulic diameter of duct, m	$\Delta T/l$	Temperature rise parameter, $K\text{-}m^2/W$
e	Rib height, m	U_b	Bottom loss coefficient, $W/m^2\text{-}K$
e/D	Relative roughness height	U_s, U_e	Side/Edge loss coefficient, $W/m^2\text{-}K$
f	Friction factor	U_l	Overall heat loss coefficient, $W/m^2\text{-}K$
h	Convective heat transfer coefficient, $W/m^2\text{-}K$	U_t	Top loss coefficient, $W/m^2\text{-}K$
I	Insolation, W/m^2	W	Width of absorber plate, m
I_{sc}	Solar constant, W/m^2	W/w	Relative roughness width
Nu	Nusselt number	V	Velocity of air in duct, m/s^2
Nu_s	Nusselt number for smooth duct	V_R	Volume of ribs per meter square of collector plate, m^3
P/e	Relative roughness pitch	V_w	Wind velocity, m/s^2
$(\Delta P)_d$	Pressure drop across duct	E_{LAT}	Exergy losses by working fluid
Pr	Prandtl number	E_{LAP}	Exergy losses by friction
Q_u	Useful heat gain, KW	E_{LA}	Exergy losses by Absorber plate
Re	Reynolds number	E_{LE}	Exergy losses by convective and radiative
T_a	Ambient temperature, K	η_{th}	Thermal efficiency
T_{fm}	Mean bulk air temperature, K	η_{eff}	Effective efficiency
T_i	Inlet air temperature, K	<i>Greek symbols</i>	
T_o	Outlet air temperature, K	α	Angle of attack($^\circ$)
T_{pm}	Mean plate temperature, K	η_c	Carnot efficiency
t_g	Thickness of glass cover, m	η_{II}	Exergetic efficiency
t_p	Thickness of absorber plate, m	η_{th}	Thermal efficiency
		$\tau\alpha$	Transmissivity-absorptivity product of glass cover

Well in thermal performance but do not affect value of convective heat transfer coefficient. It was obtained that inclination of rib results generation of vortices and secondary flow which affect value of heat transfer as compared to the continuous ribs. With the continuous research over solar air heater roughness further enhancement in effectiveness of solar air heaters, studies were performed by applying discrete rib roughness in various configurations such as V-shaped discrete (i.e., [8]), V-up and V-down discrete rib arrangements (i.e., [9]) and staggered discrete V-shaped ribs (i.e., [10]) In all these arrangements V-down discrete arrangement gives the best heat transfer performance but at the expense of large friction losses. To reduce frictional losses investigator, introduce gaps with in the roughness geometries; viz. inclined rib with gap [(i.e., [11]) V-rib with gap [(i.e., [12]) and multi V-rib with gap [(i.e., [13]) With the help of gap added advantage of secondary flow through the gaps while moving along inclined ribs and through gaps fluid accelerated which erupting the growth of boundary layer

and on the other hand friction factor encountered less then continuous ribs. Other than inclined and transverse ribs roughness arc shape roughness are also investigated to enhance the heat transfer and efficiency of solar air heater. Saini and Saini (i.e., [14]) investigated Arc shaped ribs in which enhancement obtained in order of 3.6 and 1.75 for Nusselt number (Nu) and Friction factor (f). Singh et al (i.e., [15]) investigate multi arc shaped rib roughness on the underside of absorber plate to produce an effective and economical method to improve thermal performance of solar air heater where maximum enhancement in Nusselt number (Nu) and friction factor (f) is 5.07 and 3.71 respectively for multiple arc-shaped roughness geometry as compared to smooth one. Pandey et al (i.e., [16]) experimental studied the effect of multiple arc with gap on absorber plate. The air passing through gap creates turbulence at the downstream side. Larger the value of gap width, smaller is air velocity through gap and higher the downstream disturbance area. Further increase in relative roughness pitch (p/e) number of reattachment point

diminishes hence less amount of heat transfer takes place. Various CFD investigation have reported enhancement in the thermal performance of solar air heaters by testing roughness geometries similar to those being employed for the experimental investigations by many researchers in the past. Bhagoria et al. (i.e., [17]) studied thermo hydraulic investigation of Equilateral triangular sectioned rib roughness on the absorber plate. Bhagoria et al. (i.e., [18]) studied a CFD based heat transfer and fluid flow characteristic investigation of repeated transverse square sectioned rib roughness on the absorber plate. The maximum enhancement in the Nusselt number (Nu) and friction factor (f) was found to be 2.86 & 3.14 times over the smooth duct. The exergy is given for any system at particular state is maximum extraction of work up to its thermodynamic equilibrium state with the surrounding. Exergetic concept is very important for all energy producing, energy consuming and energy conveying system. First law of thermodynamics clarifies energy analysis of thermodynamic system without any comment on its quality. Second law of thermodynamics clarify that different form of energy has different quality and energy always degrade by its quality. it is analyzed from first and second law of thermodynamics that energy and exergy based analyses has to be carried out for every energy producing, energy consuming and energy conveying system to make them more exergy efficient, which leads us to energy saving for given system. So it is the second law of thermodynamics which provide information about quality of energy. It provides the concept of available energy or exergy. With the concept it is possible to analyze means of minimizing the consumption of exergy to perform given process, thereby ensuring the most efficient possible conversion of energy for the required task. In this paper exergetic investigation has carried out on roughened solar air heater having discrete W-shape and W-shaped rib roughness on absorber plate. As well as comparative study of their performance on different flow parameters and optimum results are obtained. On the basis of design plots were also prepared in order to facilitate the designer for designing roughened solar air heater within the investigated operating and roughness parameters.

2. MATHEMATICAL MODEL AND MATLAB CODE FORMATION

In order to evaluate the exergetic efficiency (η_{eff}) of solar air heater as per Eq. (21), the calculation starts and proceeds by taking values (base and range) of systems and operating parameters as applicable for solar air heaters. The stepwise calculation procedure is given below. The range/base values of system parameters including

roughness geometries and operating parameters, as given in Table (1) for the collector under consideration, have been selected. The procedure adopted for the estimation of exergetic efficiency is same as it was given by Chamoli et al. (i.e., [19]) & Sahu et al. (i.e., [20]) and the computation procedure was carried out in MATLAB. For this purpose a step by step procedure has to be followed. The procedure for the estimation of exergetic efficiency is discussed below.

Table 1:- Typical values of system and operating parameters used in analytical calculations

Parameters	Range / Base Values
System parameters	
Collector length (L)	1.5 m
Collector width (W)	0.02 m
Collector height (H)	0.025 m
Transmittance- absorptance ($\tau\alpha$)	0.8
Emittance of glass (E_g)	0.88
Emittance of plate (E_p)	0.9
Thickness of glass cover (t_g)	0.004
Number of glass covers (N)	1
Thickness of insulation (t_i)	0.05 m
Thermal conductivity of insulation (K)	$0.037 \text{ W m}^{-1} \text{ K}^{-1}$
Relative roughness pitch (P/e)	10
Aspect ratio (W/H)	8
Angle of attack (α)	60°
Operating parameters	
Relative roughness height (e/D)	0.018-0.03375
Ambient temperature (T_a)	300 K
Wind velocity (V_w)	1 m s^{-1}
Insulation (I)	$1000,500 \text{ W m}^{-2}$
Temperature rise parameter ($\Delta T/I$) $^\circ\text{C m}^2/\text{W}$	0.005-0.035

Step 1: Area of plate is calculated as,

$$A_p = W \times H \quad (1)$$

Step 2: Hydraulic diameter of duct is calculated as

$$D = \frac{2(W \times H)}{W + H} \quad (2)$$

Step 3: A set of system parameters namely relative roughness pitch (P/e) and relative roughness height ratio (e/D) is selected.

Step 4: A set of values of design parameters namely isolation and temperature rise parameter is selected.

Step 5: The outlet temperature T_o is calculated as.

$$T_o = T_i + \frac{\Delta T}{I} I \quad (3)$$

Step 6: Inlet air temperature equals to ambient temperature. The outlet air temperature is calculated from desired temperature rise of air across the duct (ΔT) and the inlet air temperature.

Step 7: Mean film temperature is calculating as.

$$T_{fm} = \frac{T_i + T_o}{2} \quad (4)$$

Step 8: Approximate initial mean plate temperature is assumed.

$$T_{pm} = 300;$$

Step 9: Using the value of the plate temperature T_p , value of top loss coefficient, U_t is computed by using equation proposed by Klein (1975) given as, (i.e., [21])

$$U_t = [(\sigma(T_p^2 + T_g^2)(T_p + T_g) / A) + (k_a Nu / L_g)]^{-1} + B \quad (5)$$

Where,

$$A = (1 / \epsilon_p) + (1 / \epsilon_g) - 1$$

$$B = [\sigma \epsilon_g (T_p^2 + T_g^2)(T_p + T_g) + h_w]^{-1} + (t_g / k_g)$$

$$T_g = [F_1 T_p + C T_a / 1 + F_1]$$

$$F_1 = [12 \times 10^{-8} (T_a + 0.2 T_p)^+ h_w]^{-1} + 0.3 t_g / D$$

$$D = [6 \times 10^{-8} (\epsilon + 0.028)(T_p + 0.5 T_a)^3 + 0.6 L_g^{-0.2} \{(T_p - T_a) \cos \beta\}^{0.25}]^{-1}$$

$$C = [((T_s / T_a) + (h_w / 3.5)) / (1 + (h_w / 3.5))]^{-1}$$

$$T = 0.0522 (T_a)^{1.5}$$

Back loss coefficient U_b is expressed as

$$U_b = (k_i / t_i)$$

The edge loss coefficient, based on the collector area is given as; $U_e = (D t_e k_i / t_i)$

Finally,

$$U_L = U_b + U_e + U_t$$

Step 10: Useful energy gain is calculated by Hottel-Whillier-Bliss equation,

$$Q_{u1} = [I(\tau\alpha) - U_L(T_p - T_a)] A_p \quad (6)$$

Step 11: Mass flow rate is determined from the expression given as;

$$m = [Q_{u1} / C_p \Delta T] \quad (7)$$

Step 12: Reynolds number of flow of air in the duct is computed as;

$$Re = (GD / \mu) \quad (8)$$

Where, G is the mass velocity of air through the collector;

$$G = (m / W \times H)$$

Step 13: The Nusselt number (Nu) is calculated using the correlation mention in equation convective heat transfer coefficient is calculated as follows,

$$h = (Nu \times k / D) \quad (9)$$

Step 14: The plate efficiency factor is then determined as,

$$F' = h / (h + U_L) \quad (10)$$

Step 15: The heat removal factor is calculated as,

$$Fo = [(m C_p / U_L A_p) \times \exp\{J\}^{-1}] \quad (11)$$

Where,

$$J = (F' U_L A_p / m C_p)$$

Step 16: The useful heat gain, Q_{u2} is computed as,

$$Q_{u2} = Fo [I(\tau\alpha) - U_L(T_o - T_i)] A_p \quad (12)$$

Step 17: At this stage, the difference between the two values of useful heat gain Q_{u1} and Q_{u2} is checked. Ideally the two values should be same. However, if the difference in two values is more than 0.1% of Q_{u1} , then the plate temperature is modified as,

$$T_{pm} = T_a + [(I(\tau\alpha) - (Q_{u2} / A_p)) / U_L] \quad (13)$$

Step 18: Friction factor, f is calculated using the correlation developed in a previously, this is mentioned above in equation;

Step 19: Using the value of friction factor, the pressure drop (ΔP), across the duct is calculated as follow:

$$\Delta P = 4 f L \rho v^2 / 2D \quad (14)$$

Step 20: Thermal efficiency is calculated

$$\eta_{th} = Fo [\tau\alpha - U_L(T_{fm} - T_a) / I] \quad (15)$$

Step 21: The effective efficiency, η_{eff} is calculated as;

$$\eta_{eff} = [(Q_{u2} - (P_m / c)) / I A_p] \quad (16)$$

Step 22: Logarithmic mean fluid temperature (T_{fm}) is calculated as follow,

$$T_{fm} = [(T_o - T_a) / (\ln(T_o / T_a))] \quad (17)$$

Step 23: Carnot efficiency based on logarithmic mean fluid temperature as source and ambient temperature as sink can be calculated as follows,

$$\eta_c = [1 - (T_a / T_{fm})] \quad (18)$$

The maximum exergy efficiency can be obtained by minimizing exergy losses and maximizing the net exergy flow. The components of exergy losses are (i.e., [22])

Step 24: Net exergy flow is calculated as

$$E_n = I A_p \eta_{th} \eta_c - P_m (1 - \eta_c) \quad (19)$$

Step 25: Exergy input is calculated as;

$$E_s = I A_p (1 - (T_a / T_{sun})) \quad (20)$$

Step 26: Exergetic efficiency is calculated as;

$$\eta_{exe} = (E_n / E_s) \quad (21)$$

Step 27: Optical losses are calculated as:

$$E_{LO} = I A_p \eta_{exe} (1 - \tau\alpha) \quad (22)$$

Step 28: Exergy losses by absorption of irradiation by the absorber are calculated as:

$$E_{LA} = IA_p \tau \alpha \eta_{exe} - (1 - (T_a / T_{pm})) \quad (23)$$

Step 29: Exergy losses by both radiative and convective heat transfer from the absorber to the atmosphere are calculated by:

$$E_{LE} = U_{LA} p (T_{pm} - T_a) (1 - (T_a / T_{pm})) \quad (24)$$

Step 30: Exergy losses by the heat transfer to the working fluid are calculated by:

$$E_{LAT} = A_p \eta_{th} \{ (T_a / T_{fm}) - (T_a / T_{pm}) \} \quad (25)$$

Step 31: Exergy losses by friction are determined by:

$$E_{LAP} = [(m / \rho) \Delta P (T_a / T_{fm})] \quad (26)$$

The experimental investigation had been carried out by investigator and on that Nusselt number and friction factor correlations were obtained, which were used in this paper for further calculation purpose of exergetic efficiency. Correlations for Nusselt number (Nu) and Friction factor (f) for discrete W-shaped rib roughness and W-shaped rib roughness; Re = 4000–14,000 and relative roughness height (e/D) is as follows:

Correlation for W-shaped rib roughness (i.e., [23])

$$Nu = 0.0613 \times Re^{0.9079} \times (e / D)^{0.4487} \times (alp / 60)^{0.1331} \times \exp((-0.5307 \times (\log(alp / 60)^2))) \quad (27)$$

$$f = 0.6182 \times Re^{0.2254} \times (e / D)^{0.04622} \times (alp / 60)^{0.0817} \times \exp((-0.28 \times (\log(alp / 60)^2))) \quad (28)$$

Correlation for discrete W-shaped rib roughness: (i.e.,[24])

$$Nu = 0.105 \times Re^{0.873} \times (e / D)^{0.453} \times (alp / 60) - 0.081 \times \exp((-0.059 \times (\log(alp / 60)^2))) \quad (29)$$

$$f = 0.568 \times Re^{-0.40} \times (e / D)^{0.49} \times (alp / 60)^{-0.081} \times \exp((-0.579 \times (\log(alp / 60)^2))) \quad (30)$$

3. MATLAB SIMULATION RESULTS

3.1. Exergetic efficiency (η_{II})

The exergy of a system is the maximum useful work possible during a process up to the equilibrium process, but we always deal with exergetic efficiency. At lower temperature rise parameters the negative value of exergetic efficiency occurred because of higher mass flow rate and insufficient temperature rise but after this exergetic efficiency reaches maximum at certain value of

temperature rise parameter and then start decreasing. It happens because of lower convective heat transfer coefficient (h) value of air. For different values of relative roughness height (e/D) shown in Figure (4.14) the lower exergetic efficiency found for relative roughness height (e/D) value of 0.018 and high exergetic efficiency found for relative roughness height (e/D) value of 0.03375 at angle of attack (α) value of 60° as shown in (Fig. 1).

3.2. Exergy losses by absorber (E_{LA})

Exergetic losses by absorber are due to insufficient temperature rise of mean plate temperature. At angle of attack (α) of 60° maximum decrement gap of exergetic losses by absorber are obtained at relative roughness height of 0.018 for W-shape while minimum decrement gap obtained for discrete W-shape roughness at relative roughness height of 0.0375 in (Fig. 2). This is due to the fact that at relatively higher values of relative roughness height, the re-attachment of free shear layer might not occur. As lower relative roughness height value does not create as much disturbance within the fluid flow which results less heat gain by flowing fluid and maximum losses on absorber.

3.3. Exergy losses by friction (E_{LAP})

A higher exergy loss due to friction is because of higher mass flow rate associated with lower temperature rise parameter at higher Reynolds number in the beginning of fluid flow in the duct. The maximum amount of frictional exergetic losses are obtained at angle of attack (α) of 60°. At this angle of attack flow separation in secondary flow as result of discrete W-shaped rib roughness and movement of resulting vortices combine to yield an optimum value as shown in (Fig. 3). A higher relative roughness height pertain higher friction factor because of higher level of turbulence in the flow.

3.4. Exergy losses by working fluid (E_{LAT})

Increase in temperature rise parameter ($\Delta T/I$) leads to higher amount of irreversibility and hence higher exergy losses. Absorber plate temperature increases with an increase of temperature rise parameter ($\Delta T/I$). Thus maximum exergetic losses result from higher value of temperature rise parameter ($\Delta T/I$). Value of exergy losses by working fluid (E_{LAT}) with temperature rise parameter increase for relative roughness height (e/D) 0.018 but after a certain point it decreases and found maximum for relative roughness height (e/D) 0.03375 as shown in (Fig. 4) for angle of attack (α) of 60°.

3.5. Exergy losses by convective and radiative (E_{LE})

The losses are occurred because of the higher temperature difference between absorber plate and the environment. As the absorber plate temperature

continuously increasing, the losses due to the radiation become more dominant than conductive losses. Thus minimum exergy losses as a result of heat transfer to environment occur for minimum temperature rise parameter. From Figure (4.11) the higher value of E_{LE} found at relative roughness height (e/D) value of 0.018 and minimum for relative roughness height (e/D) value of 0.0375 at angle of attack (α) of 60° as shown in (Fig. 5).

3.6. Thermal efficiency (η_{th})

Thermal efficiency is defined as the ratio of useful heat gain to the intensity of radiation incident on the heat transfer surface. So it is clear that the roughened surface responsible to maximize the useful heat gain will have maximum thermal efficiency. Thermal efficiency decreases with increase in temperature rise parameter ($\Delta T/I$). The minimum decrement in thermal efficiency obtained by discrete W-shaped rib roughness at relative roughness height (e/D) of 0.03375 as shown in (Fig. 6).

3.7. Effective efficiency (η_{eff})

Effective efficiency defines as difference between useful heat gain and heat losses to the product of total isolation incident on solar absorber. Initially losses are minimum so the effective efficiency achieved maximum and after that it keep on decreasing because of losses as shown in (Fig. 7).

It can be analysed from the (Fig. 8) that the value of exergetic efficiency varies with Reynolds number (Re) up to <6000 and relative roughness height (e/D) = 0.03375 have highest exergetic efficiency for Reynolds no. (Re) < 6000 . Exergetic efficiency (η_{exe}) started decreasing after > 6000 because of thermal energy transfer domination over the pumping power consumption. The smooth plate solar air heater is having a low value of exergetic efficiency (η_{exe}) for all values of Reynolds number (Re) as compared to the roughened solar air heater duct.

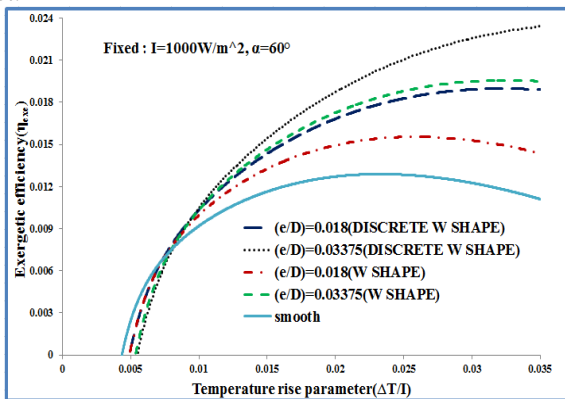


Fig.1 - Variation of (η_{exe}) with temperature rise parameter for angle of attack (α) of 60°

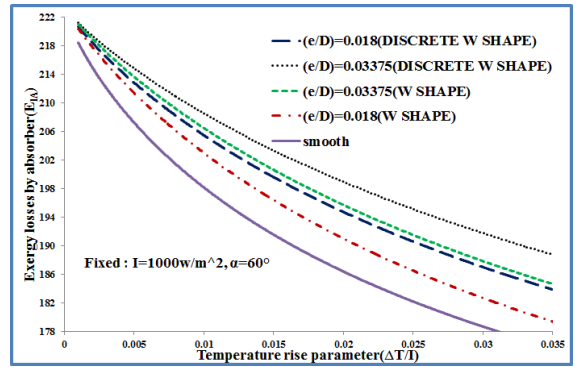


Fig.2 - Variation of (E_{LA}) with temperature rise parameter for angle of attack (α) of 60°

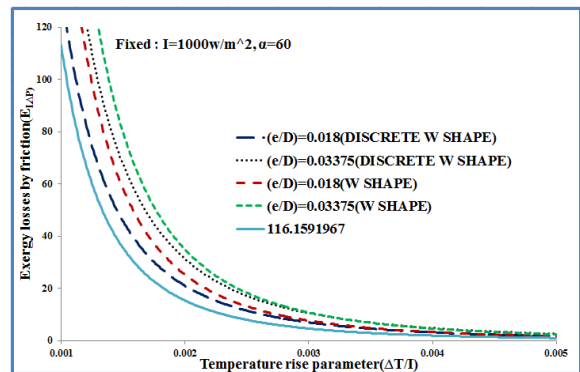


Fig.3 - Variation of (E_{LAP}) with temperature rise parameter for angle of attack (α) of 60°

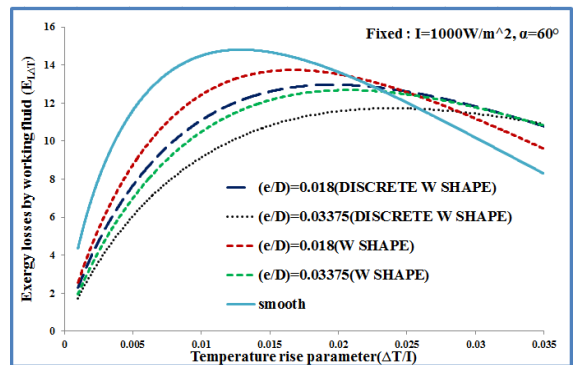


Fig.4 - Variation of (E_{LAT}) with temperature rise parameter for angle of attack (α) of 60°

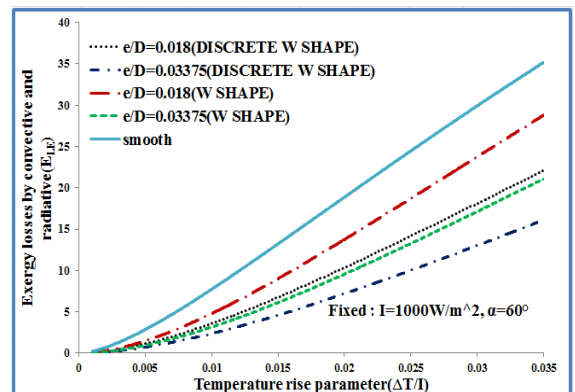


Fig.5 - Variation of (E_{LE}) with temperature rise parameter for angle of attack (α) of 60°

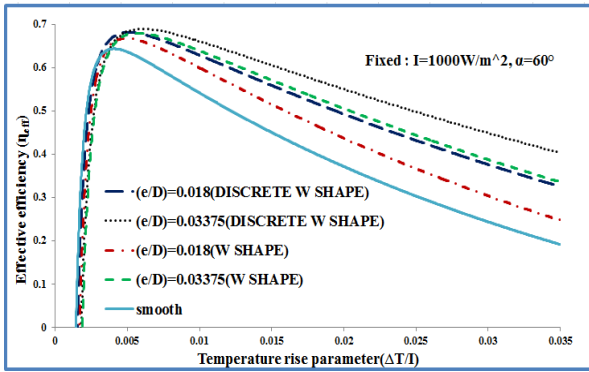


Fig.6 - Variation of effective efficiency (η_{eff}) with temperature rise parameter ($\Delta T/I$) for angle of attack (α) 60°

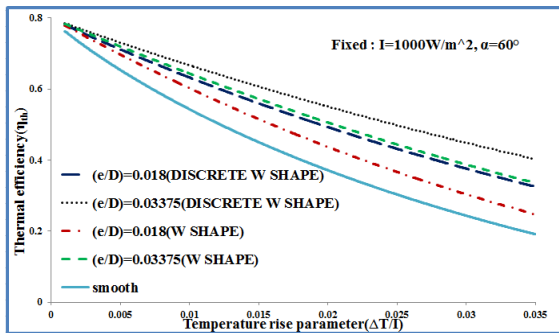


Fig.7 - Effect of temperature rise parameter ($\Delta T/I$) on thermal efficiency (η_{th})

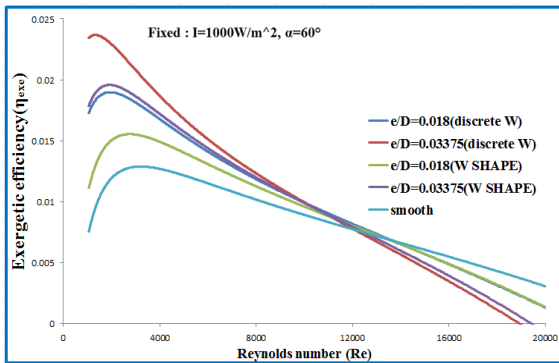


Fig.8 - Effect of temperature rise parameter ($\Delta T/I$) on Reynolds number (Re)

4. OPTIMIZATION OF ROUGHNESS PARAMETERS

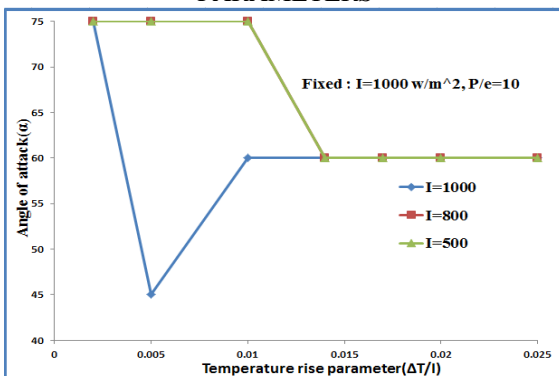


Fig.9 - Variation of angle of attack (α) with temperature rise parameter for different intensity of radiation for discrete W-shaped rib roughness

The optimum values plots of relative roughness height (e/D), and relative angle of attack (α) that correspond to maximum exergetic efficiency (η_{ex}) for a given value of temperature rise parameter ($\Delta T/I$) are shown in (Fig. 9), (Fig. 10), (Fig. 11) and (Fig. 12) respectively. From the plots it is concluded that the optimum value of relative roughness height (e/D) is 0.03375 for W-shape rib and discrete W-shape rib roughness for different value of insolation (I) and optimum value of angle of attack (α) is 60° for W-shape rib and discrete W-shape rib roughness for different value of insolation (I).

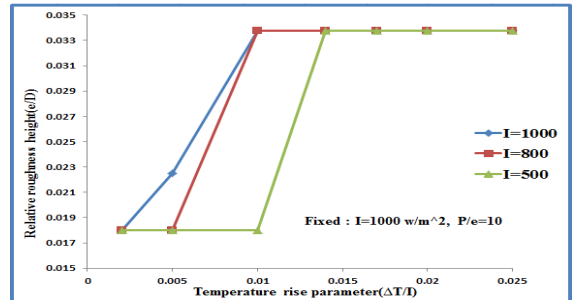


Fig.10 - Variation of relative roughness height (e/D) with temperature rise parameter for different intensity of radiation for discrete W-shaped rib roughness

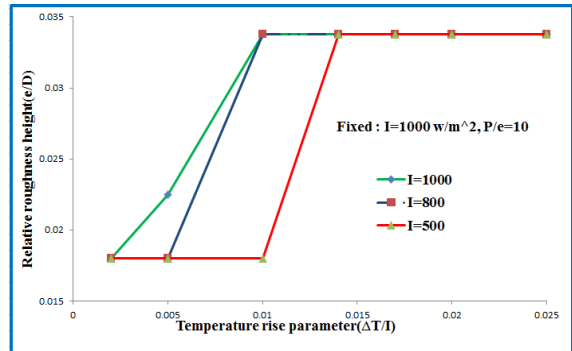


Fig.11 - Variation of relative roughness height (e/D) with temperature rise parameter for different intensity of Radiation for W-shaped rib roughness

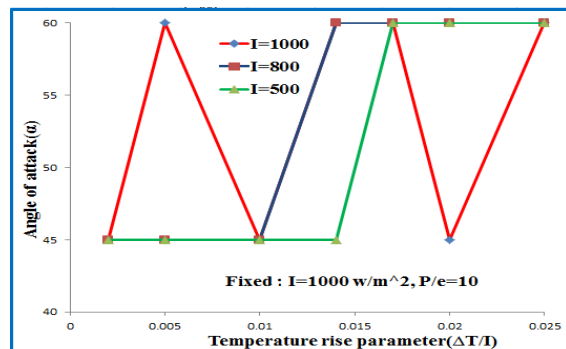


Fig.12 - Variation of angle of attack (α) with temperature rise parameter ($\Delta T/I$) for different intensity of radiation for W-shaped rib roughness

5. CONCLUSION

This study was taken up with purpose of heat transfer in W-shaped and discrete W-shaped rib as roughness element of the duct of solar air heater. This is considered as an important objective throughout the study of solar air heater. An analytical model based upon MATLAB programming has been developed based upon which the exergetic efficiency criteria has been used for optimization of roughness parameters for specified operating condition of solar air heater.

There is significant increase in exergetic efficiency (η_{exe}) of solar air heater with arc shaped wire rib roughened absorber plate. The exergetic efficiency enhances up to 63% over the smooth plate solar air heater. The maximum exergetic efficiency for the relative roughness pitch (p/e) is found at relative roughness height (e/D) of 0.03375, and angle of attack (α) value of 60° for discrete W-shaped rib roughness respectively with variation of temperature rise parameter ($\Delta T/I$) as compared to the W-shaped rib roughness. Exergetic efficiency obtained maximum at angle of attack (α) of 60° followed by angle of attack (α) of 45° and then angle of attack (α) of 75° for both W-shaped rib roughness and discrete W-shaped rib roughness. At higher Reynolds number (Re) above 20,000, exergetic efficiency of roughened solar air heater becomes negative and thus it is not desirable to run the system beyond this Reynolds number. Different exergetic components of artificially roughened solar air heater with W-shaped and discrete W-shaped rib for different values of system and operating parameters have been concluded. Different exergetic factors determination of the set of optimum values of the roughness parameters (Relative roughness height (e/D), and flow angle of attack (α)) to result in best exergetic performance of solar air heater has been carried out during the study. The study will help the designer in future to select optimum roughness geometry that bears best performance from the design plots and tables.

6. REFERENCES

- [1] Mittal, M.K., Varun, Saini, R.P., Singal, S.K., 2007. Effective efficiency of solar air heaters having different types of roughness element on the absorber plate. *Energy* 32, 739–745.
- [2] K. Prasad, S.C. Mullick, Heat transfer characteristics of a solar air heater used for drying purposes, *Appl. Energy* 13 (1983) 83e93.
- [3] B.N. Prasad, J.S. Saini, Effect of artificial roughness on heat transfer and friction factor in a solar air heater, *Sol. Energy* 41 (1988) 555e560
- [4] A.M.E. Momin, J.S. Saini, S.C. Solanki, Heat transfer and friction in solar air heater duct with V-shaped rib roughness on absorber plate, *Int. J. Heat Mass Transf.* 45 (2002) 3383e3396.
- [5] R. Karwa, Experimental studies of augmented heat transfer and friction in asymmetrically heated rectangular ducts with ribs on the heated wall in transverse, inclined, v-continuous and v-discrete pattern, *Int. Common. Heat Mass Transf.* 30(2003) 241e250.
- [6] S.K. Saini, R.P. Saini, Development of correlations for Nusselt number and friction factor for solar air heater with roughened duct having arc-shaped wire as artificial roughness, *Sol. Energy* 82 (2008) 1118e1130.
- [7] V.S. Hans, R.P. Saini, J.S. Saini, Heat transfer and friction factor correlations for a solar air heater duct roughened artificially with multiple V-ribs, *Sol. Energy* 84 (2010) 898e911.
- [8] R. Karwa, R.D. Bairwa, B.P. Jain, N. Karwa, Experimental study of the effects of rib angle and discretization on the heat transfer and friction in an asymmetrically heated rectangular duct, *J. Enhanc. Heat Transf.* 12 (4) (2005) 343e355.
- [9] R. Karwa, Experimental studies of augmented heat transfer and friction in asymmetrically heated rectangular ducts with ribs on the heated wall in transverse, inclined, v-continuous and v-discrete pattern, *Int. Commun. Heat Mass Transf.* 30 (2003) 241e250
- [10] K.B. Mulluwork, Investigations on Fluid Flow and Heat Transfer in Roughened Absorber Solar Heaters, Ph.D. Dissertation, IIT, Roorkee, 2000.
- [11] K.R. Aharwal, B.K. Gandhi, J.S. Saini, Heat transfer and friction characteristics of solar air heater ducts having integral inclined discrete ribs on absorber plate, *Int. J. Heat Mass Transf.* 52 (2009) 5970e5977.
- [12] S. Singh, S. Chander, J.S. Saini, Heat transfer and friction factor of discrete V down rib roughened solar air heater ducts, *J. Renew. Sustain. Energy* 3 (1)(2011) 013108e013117.
- [13] K. Anil, R.P. Saini, J.S. Saini, Experimental investigations on thermo-hydraulic performance due to flow-attack-angle in multiple V-down ribs with gap in a rectangular duct of solar air heaters, *J. Sustain. Energy & Environ.* 4 (2013) 1e7
- [14] K. Anil, R.P. Saini, J.S. Saini, Experimental investigations on thermo-hydraulic performance due to flow-attack-angle in multiple V-down ribs with gap in a rectangular duct of solar air heaters, *J. Sustain. Energy & Environ.* 4 (2013) 1e7.
- [15] Anil P. Singh, Varun, Siddhartha, "Heat transfer and friction factor correlations for multiple arc shape roughness elements on the absorber plate used in solar air heaters", *Experimental Thermal and Fluid Science* 54 (2014) 117–126
- [16] N.K. Pandey, V.K. Bajpai, Varun, "Experimental investigation of heat transfer augmentation using multiple arcs with gap on absorber plate of solar air heater", *Solar Energy* 134 (2016) 314–326
- [17] Anil Singh Yadav, J.L. Bhagoria, "A CFD based thermo-hydraulic performance analysis of an artificially roughened solar air heater having equilateral triangular sectioned rib roughness on the absorber plate", *International Journal of Heat and Mass Transfer* 70 (2014) 1016–1039
- [18] Anil Singh Yadav, J.L. Bhagoria, "A numerical investigation of square sectioned transverse rib roughened solar air heater", *International Journal of Thermal Sciences* 79 (2014) 111e131
- [19] Sunil Chamoli, N. Thakur, Performance study of solar air heater duct having absorber plate with V down perforated baffles, *Songklanakarian journal of science and technology*, 36 (2) (2014) 201-208.
- [20] Mukesh Kumar Sahu, Radha Krishna Prasad, Exergy based performance evaluation of solar air heater with arc-shaped wire roughened absorber plate, *Renewable Energy* 96 (2016) 233e243.
- [21] S. J. Kline, F.A. McClintock. Describing uncertainties insingle sample experiments, *Mechanical engineering* 75 (1953): 3-8.
- [22] K. Altfeld, W. Leiner, M. Fiebig, Second law optimization of flat-plate solar air heaters part I: the concept of net exergy flow and the modeling of solar air heaters, *Sol. Energy* 41 (1988) 127e132.
- [23] Atul Lanjewar*, J.L. Bhagoria, R.M. Sarviya, Heat transfer and friction in solar air heater duct with W-shaped rib roughness on absorber plate, *Energy* 36 (2011) 4531e4541
- [24] Arvind Kumar *, J.L. Bhagoria, R.M. Sarviya, Heat transfer and friction correlations for artificially roughened solar air heater duct with discrete W-shaped ribs, *Energy Conversion and Management* 50 (2009) 2106–2111

FLOWCHART

